J|A|C|S
ARTICLES

Published on Web 11/30/2009

Chemical Double Mutant Cycles for the Quantification of Cooperativity in H-Bonded Complexes

Amaya Camara-Campos, Daniele Musumeci, Christopher A. Hunter,* and Simon Turega

Krebs Institute, Department of Chemistry, University of Sheffield, Sheffield S3 7HF, United Kingdom

Received October 1, 2009; E-mail: c.hunter@sheffield.ac.uk

Abstract: Chemical double mutant cycles have been used in conjunction with new H-bonding motifs for the quantification of chelate cooperativity in multiply H-bonded complexes. The double mutant cycle approach specifically deals with the effects of substituents, secondary interactions, and allosteric cooperativity on the free energy contributions from individual H-bond sites and allows dissection of the free energy contribution due to chelate cooperativity associated with the formation of intramolecular noncovalent interactions. Two different doubly H-bonded motifs were investigated in carbon tetrachloride, chloroform, 1,1,2,2-tetrachloroethane, and cyclohexane, and the results were similar in all cases, with effective molarities of 3−33 M for formation of intramolecular H-bonds. This corresponds to a free energy penalty of 3−9 kJ mol^{-1} for formation of a bimolecular complex in solution, which is consistent with previous estimates of 6 kJ mol^{-1}. This result can be used in conjunction with the H-bond parameters, α and β, to make a reasonable estimate of the stability constant for formation of a multiply H-bonded complex between two perfectly complementary partners, or to place an upper limit on the stability constant expected for a less complementary system.

Introduction

The development of a quantitative understanding of molecular interactions is the key to harnessing the potential of molecular recognition in areas of molecular engineering such as nanotechnology and drug design.[1] At the level of simple functional group interactions in nonpolar solvents, the principles are reasonably well-established: the more polar are the functional groups, the stronger are the interactions.[1,2] However, in systems that feature multiple interaction sites, it is more difficult to make predictions. In general, the more interactions there are, the more stable is the complex, but the extent to which cooperativity between multiple interaction sites is expressed is not well-understood at a quantitative level.[3] This type of chelate cooperativity is experimentally quantified by the effective molarity, EM, which is a measure of the increased probability of intramolecular contacts relative to intermolecular contacts.[4] However, estimates of effective molarities for noncovalent intramolecular interactions span over 10 orders of magnitude, so it is hazardous to try to make quantitative predictions of the binding properties of cooperative systems that are common in, for example, supramolecular self-assembly, macromolecular, and biomolecular structures.[5]

One of the problems with experimental quantification of chelate cooperativity is that it is necessarily found in relatively complex systems, where there are multiple noncovalent interactions that are difficult to dissect. Even for apparently simple systems, such as the DNA base-pair type H-bonded complexes that have been extensively studied, a straightforward separation of the contributions to binding is not possible: there are secondary electrostatic interactions between the H-bonding functional groups that are very close in space, and this contribution is difficult to measure directly; there are through-bond polarization effects that make it practically impossible to identify a good reference system, where a single isolated H-bond can be characterized; if an appropriate reference complex that makes only one H-bond can be identified, the stability of this complex is unlikely to be sufficient to allow accurate determination of the association constant.[6] These problems can be avoided in carefully designed systems that feature very strong binding interactions located at well-defined and well-separated sites, and so chelate cooperativity can be quantified more

(1) (a) Meyer, E. A.; Castellano, R. K.; Diederich, F. *Angew. Chem., Int. Ed.* **2003**, *432*, 1210–1250. (b) Schneider, H.-J. *Angew. Chem., Int. Ed.* **2009**, *48*, 3924–3977. (c) Kay, E. R.; Leigh, D. A.; Zerbetto, F. *Angew. Chem., Int. Ed.* **2007**, *46*, 72–191.

(2) (a) Abraham, M. H.; Platts, J. A. *J. Org. Chem.* **2001**, *66*, 3484–3491. (b) Hunter, C. A. *Angew. Chem., Int. Ed.* **2004**, *43*, 5310–5324.

(3) (a) Shinkai, S.; Ikeda, M.; Sugasaki, A.; Takeuchi, M. *Acc. Chem. Res.* **2001**, *34*, 494–503. (b) Badjic, J. D.; Nelson, A.; Cantrill, S. J.; Turnbull, W. B.; Stoddart, J. F. *Acc. Chem. Res.* **2005**, *38*, 723–732. (c) Mulder, A.; Huskens, J.; Reinhoudt, D. N. *Org. Biomol. Chem.* **2004**, *2*, 3409–3402. (d) Mammen, M.; Choi, S.-K.; Whitesides, G. M. *Angew. Chem., Int. Ed.* **1998**, *37*, 2754–2794. (e) Ercolani, G. *J. Am. Chem. Soc.* **2003**, *125*, 16097–16103. (f) Williams, D. H.; Stephens, E.; O'Brien, D. P.; Zhou, M. *Angew. Chem., Int. Ed.* **2004**, *43*, 6596–6616. (g) Calderone, C. T.; Williams, D. H. *J. Am. Chem. Soc.* **2001**, *123*, 6262–6267. (h) Hamacek, J.; Borkovec, M.; Piguet, C. *Dalton Trans.* **2006**, 1473–1490. (i) Kaiser, T. E.; Stepanenko, V.; Würthner, F. *J. Am. Chem. Soc.* **2009**, *131*, 2719–6712. (j) Chekmeneva, E.; Hunter, C. A.; Packer, M. J.; Turega, S. M. *J. Am. Chem. Soc.* **2008**, *130*, 17718–17725. (k) Hunter, C. A.; Tomas, S. *Chem. Biol.* **2003**, *10*, 1023–1032. (l) Tobey, S. L.; Anslyn, E. V. *J. Am. Chem. Soc.* **2003**, *125*, 10963–10970. (m) Hughes, A. D.; Anslyn, E. V. *Proc. Natl. Acad. Sci. U.S.A.* **2007**, *104*, 6538–6543. (n) Jadhav, V. D.; Schmidtchen, F. P. *Org. Lett.* **2006**, *8*, 2329–2332.

(4) (a) Adamson, A. W. *J. Am. Chem. Soc.* **1954**, *76*, 1578–1579. (b) Jencks, W. P. *Proc. Natl. Acad. Sci. U.S.A.* **1981**, *88*, 4046–4050. (c) Zhang, B.; Breslow, R. *J. Am. Chem. Soc.* **1993**, *115*, 9353–9354.

10.1021/ja9083495 © **2009 American Chemical Society**

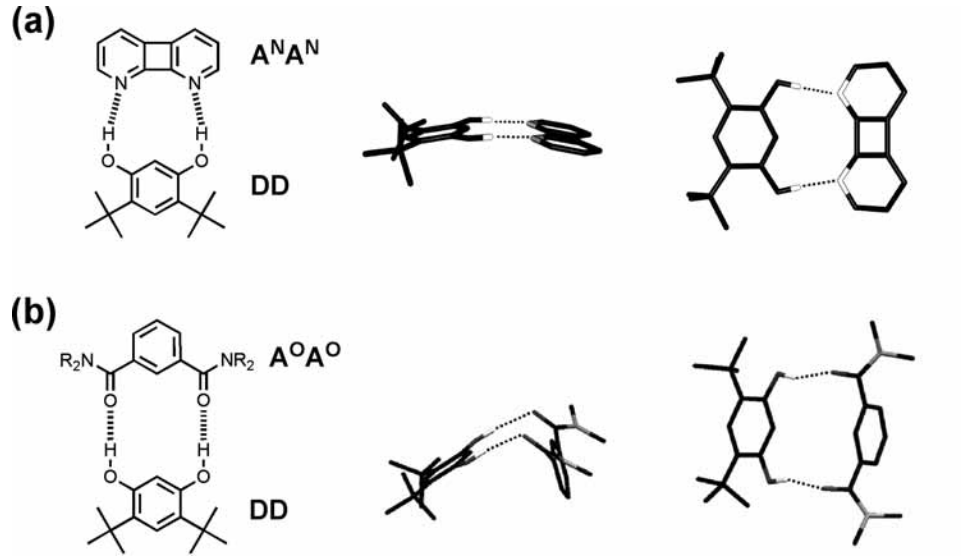

Figure 1. Proposed structures of complexes for studying H-bond cooperativity: (a) $\mathbf{A^NA^N \cdot DD}$ and (b) $\mathbf{A^OA^O \cdot DD}$ (R = 2-ethylhexyl). Two views of the molecular mechanics structures obtained by energy minimization using the OPLS force-field in Macromodel are also shown.[10]

routinely in complexes that are bound via metal−ligand interactions.[7] Here, we describe a new H-bond motif that is designed to allow accurate quantification of chelate cooperativity in a H-bonded complex using chemical double mutant cycles.

Results and Discussion

Approach. Two different types of complex were chosen for investigation (Figure 1). By using a **DD·AA** H-bonding motif and molecules that contain no additional H-bonding sites, complications associated with self-interaction are minimized. Although the oxygen of phenol is a H-bond acceptor, it is not a very good one ($\beta = 2.7$),[8] so self-association is negligible at millimolar concentrations. Phenol is one of the strongest H-bond donor functional groups ($\alpha \approx 4$), and amides and pyridines are very good H-bond acceptors ($\beta \approx 8$ and 7, respectively), which ensures that reference complexes featuring a single H-bond will be sufficiently stable to measure accurate association constants.[2] The complexes in Figure 1 both feature two H-bonding interactions that are separated by sufficient distance to ensure that the secondary electrostatic interactions that usually complicate the analysis of multiply H-bonded complexes are minimized.[6] The components of the complexes all have limited torsional flexibility, which should minimize contributions from changes in conformational entropy on binding.[9] The separation of the H-bond acceptor sites on 1,8-diazabiphenylene and the bisamide differs slightly, and molecular mechanics calculations suggest that there are differences between the complementarity of the two **AA·DD** H-bonding motifs. 1,8-Diazabiphenylene can make two H-bonds with resorcinol in a planar complex (Figure 1a), whereas the bisamide has to adopt a tilted geometry to make two interactions (Figure 1b). In addition, the bisamide has more conformational flexibility than 1,8-diazabiphenylene, which could affect cooperativity between the two binding sites.

The chelate cooperativity in these systems can be quantified by comparing the stability of the doubly H-bonded complexes with a set of reference complexes that feature only single point binding interactions. Pyridine (designated $\mathbf{A^N}$), monoamide ($\mathbf{A^O}$), and 4-*t*-butylphenol (**D**) were used as monofunctional reference compounds for 1,8-diazabiphenylene ($\mathbf{A^NA^N}$), bisamide ($\mathbf{A^OA^O}$), and resorcinol (**DD**), respectively (Figure 2). Compounds **D**, **DD**, $\mathbf{A^N}$, and $\mathbf{A^NA^N}$ are commercially available, and the amides were synthesized in one-step reactions (see Supporting Information). The chemical double mutant cycle in Figure 3 illustrates the use of the reference compounds to determine the free energy contribution associated with the intramolecularity of the second H-bond in the doubly H-bonded complexes.[11] Changing the substituents on the aromatic rings affects the H-bonding properties of the key functional groups. For example, *t*-butyl substituents are known to perturb the H-bond properties of

(5) (a) Page, M. I.; Jencks, W. P. *Proc. Natl. Acad. Sci. U.S.A.* **1971**, *68*, 1678–1683. (b) Böhm, H.-J. *J. Comput.-Aided Mol. Des.* **1994**, *8*, 243–256. (c) Searle, M. S.; Williams, D. H.; Gerhard, U. *J. Am. Chem. Soc.* **1992**, *114*, 10697–10704.
(6) (a) Quinn, J. R.; Zimmerman, S. C.; Del Bene, J. E.; Shavitt, I. *J. Am. Chem. Soc.* **2007**, *129*, 934–941. (b) Jorgensen, W. L.; Pranata, J. *J. Am. Chem. Soc.* **1990**, *112*, 2008–2010. (c) Sartorius, J.; Schneider, H.-J. *Chem.-Eur. J.* **1996**, *2*, 1446–1452. (d) Beijer, F. H.; Sijbesma, R. P.; Kooijman, H.; Spek, A. L.; Meijer, E. W. *J. Am. Chem. Soc.* **1998**, *120*, 6761–6769.
(7) (a) Taylor, P. N.; Anderson, H. L. *J. Am. Chem. Soc.* **1999**, *121*, 11538–11545. (b) Screen, T. E. O.; Thorne, J. R. G.; Denning, R. G.; Bucknall, D. G.; Anderson, H. L. *J. Mater. Chem.* **2003**, *13*, 2796–2808. (c) Camara-Campos, A.; Hunter, C. A.; Tomas, S. *Proc. Natl. Acad. Sci. U.S.A.* **2006**, *103*, 3034–3038. (d) Baldini, L.; Ballester, P.; Casnati, A.; Gomila, R. M.; Hunter, C. A.; Sansone, F.; Ungaro, R. *J. Am. Chem. Soc.* **2003**, *125*, 14181–14189. (e) Chi, X. L.; Guerin, A. J.; Haycock, R. A.; Hunter, C. A.; Sarson, L. D. *Chem. Commun.* **1995**, 2563–2565.
(8) Abraham, M. H.; Grellier, P. L.; Prior, D. V.; Morris, J. J.; Taylor, P. J. *J. Chem. Soc., Perkin Trans. 2* **1990**, 521–529.
(9) Searle, M. S.; Williams, D. H. *J. Am. Chem. Soc.* **1992**, *114*, 10690–10697.
(10) Mohamadi, F.; Richard, N. G. J.; Guida, W. C.; Liskamp, R.; Lipton, M.; Caufield, C.; Chang, G.; Hendrickson, T.; Still, W. C. *J. Comput. Chem.* **1990**, *11*, 440.
(11) (a) Cockroft, S. L.; Hunter, C. A. *Chem. Soc. Rev.* **2007**, *36*, 172–188. (b) Carver, F. J.; Hunter, C. A.; Jones, P. S.; Livingstone, D. J.; McCabe, J. F.; Seward, E. M.; Tiger, P.; Spey, S. E. *Chem.-Eur. J.* **2001**, *7*, 4854–4862. (c) Carver, F. J.; Hunter, C. A.; Livingstone, D. J.; McCabe, J. F.; Seward, E. M. *Chem.-Eur. J.* **2002**, *8*, 2848–2859. (d) Hunter, C. A.; Low, C. M. R.; Rotger, C.; Vinter, J. G.; Zonta, C. *Proc. Natl. Acad. Sci. U.S.A.* **2002**, *99*, 4873–4876. (e) Cockroft, S. L.; Hunter, C. A.; Lawson, K. R.; Perkins, J.; Urch, C. J. *J. Am. Chem. Soc.* **2005**, *127*, 8594–8595. (f) Cockroft, S. L.; Perkins, J.; Zonta, C.; Adams, H.; Spey, S. E.; Low, C. M. R.; Vinter, J. G.; Lawson, K. R.; Urch, C. J.; Hunter, C. A. *Org. Biomol. Chem.* **2007**, *5*, 1062–1080.

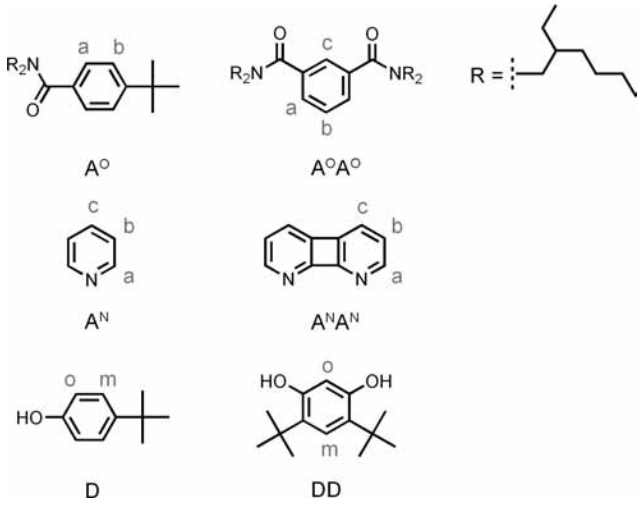

Figure 2. Compound used in ^{1}H NMR titrations and the proton labeling scheme.

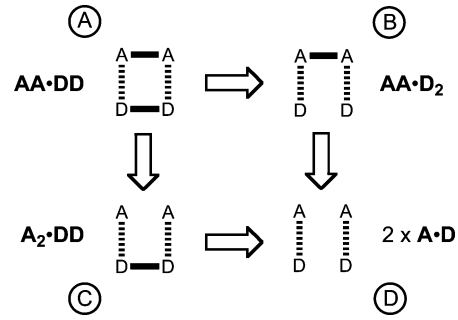

Figure 3. Chemical double mutant cycle to quantify the free energy benefit associated with the intramolecularity of the second H-bond in the **AA·DD** complex, state A.

phenols: for phenol $\alpha = 3.8$, for 4-*t*-butylphenol $\alpha = 3.6$, and for 2-*t*-butylphenol $\alpha = 3.4$.[12] The reference complexes allow us to quantify these effects in the system of interest and thereby measure their contribution to the observed stability of the **AA·DD** complex. Thus, the difference between the stabilities of complexes **A·D** and **A$_2$·DD** can be used to measure the difference between the H-bond donor properties of the phenol and resorcinol. The difference between the stabilities of complexes **A^O·D** and **A^{O}A^O·D$_2$** can be used to measure the difference between the H-bond acceptor properties of the mono- and bisamide. These comparisons also quantify any allosteric cooperativity present in the complexes (see ref 13 for a discussion of the differences between allosteric and chelate cooperativity).[4] For example, binding at one hydroxyl on resorcinol (**DD**) may polarize the other hydroxyl group and cause changes in the strength of the second H-bond. The magnitude of this allosteric effect is a contribution to the difference between the stability of **A·D** and **AA·D$_2$**, and so it does not perturb the measurement of chelate cooperativity. The double mutant cycle in Figure 3 quantifies and eliminates all of these secondary and allosteric effects to obtain a direct measurement of the free energy benefit associated with a cooperative intramolecular H-bond interaction.

This double mutant cycle differs from those that we have used previously to quantify functional group interactions. Here, the chemical mutations correspond to removal of the covalent connectivity between interaction sites rather than removal of the interactions sites themselves. Thus, the double mutant state **D** is two unconnected 1:1 complexes rather than a single complex (Figure 3), and the free energy of state **D**, ΔG°_D, is twice the free energy for formation of the singly H-bonded **A·D** complex, $2\Delta G^\circ$(**A·D**). The double mutant cycle measurement of cooperativity, $\Delta\Delta G^\circ$, is given by eq 1.[11]

$$\begin{aligned}\Delta\Delta G^\circ &= \Delta G^\circ_A - \Delta G^\circ_B - \Delta G^\circ_C + \Delta G^\circ_D \\ &= \Delta G^\circ(\mathbf{AA{\cdot}DD}) - \Delta G^\circ(\mathbf{AA{\cdot}D_2}) - \Delta G^\circ(\mathbf{A_2{\cdot}DD}) + \\ &\qquad 2\Delta G^\circ(\mathbf{A{\cdot}D}) \end{aligned} \quad (1)$$

The number of functional group interactions in each of the states A, B, C, and D in Figure 3 is the same, but the stoichiometries differ, and so $\Delta\Delta G^\circ$ is actually a measure of the effective molarity (EM) for the intramolecular interaction in the doubly H-bonded complex, rather than the strength of the intramolecular H-bond. Equation 1 can be rewritten in terms of association constants for the four different states, A, B, C, and D in Figure 3, to give eq 2, which we can recognize as the conventional definition of EM.[4]

$$2\mathrm{EM} = \frac{K_A K_D}{K_B K_C} = \frac{K(\mathbf{AA{\cdot}DD})K^2(\mathbf{A{\cdot}D})}{K(\mathbf{AA{\cdot}D_2})K(\mathbf{A_2{\cdot}DD})} = e^{-\Delta\Delta G^\circ/RT} \quad (2)$$

where K_D is K^2(**A·D**), because there are two 1:1 complexes in this state, and the statistical factor of 2 is applied to the effective molarity to account for the degeneracy of the two interactions in the **AA·DD** complex.

Binding Studies in Carbon Tetrachloride. The stability constants for all eight complexes were measured in carbon tetrachloride using ^{1}H NMR titration experiments. ^{1}H NMR dilution experiments indicated that self-association is not significant at the concentrations used in these experiments for any of the compounds. For the **A·D** and **AA·DD** complexes, the titration data fit well to a 1:1 binding isotherm. The behavior of the **A$_2$·DD** and **AA·D$_2$** complexes is more complicated, but the data could be fit to a 2:1 binding isotherm in all cases. The association constants and limiting complexation-induced changes in ^{1}H NMR chemical shift ($\Delta\delta$) are presented in Table 1. The amide and pyridine complexes exhibited quite different behavior and will be discussed separately.

For the amide system, the H-bond acceptor was titrated into the H-bond donor (which was the fixed concentration host), except in the case of the **A^{O}A^O·D$_2$** complex, where the solubility of phenol is sufficient to be used as the titrant (or guest). The limiting $\Delta\delta$ values for both host and guest were obtained by extrapolation of the binding isotherm, and these data provide experimental evidence for the structures of the complexes in solution. In all cases, there is a large downfield change in the chemical shift of the signal due to the **OH** protons (>+1 ppm) indicative of H-bonding interactions. The signals due to the aromatic protons on the amide ring show relatively small changes in chemical shift, while the $\Delta\delta$ values for the aromatic protons of **D** and **DD** are small and negative. In complex **A^{O}A^O·DD**, proton **o** shows a particularly large change in chemical shift, which may be due to the constrained geometry enforced by the formation of two H-bonds leading to larger aromatic ring current shifts. The three-dimensional solution structure of this complex was determined using the experimental $\Delta\delta$ values and the program *Shifty* that we have described

(12) Abraham, M. H.; Grellier, P. L.; Prior, D. V.; Duce, P. P.; Morris, J. J.; Taylor, P. J. *J. Chem. Soc., Perkin Trans. 2* **1989**, 699–711.
(13) Hunter, C. A.; Anderson, H. L. *Angew. Chem., Int. Ed.* **2009**, *40*, 2678–2686.

Table 1. Association Constants and Limiting Complexation-Induced Changes in Chemical Shift from ^{1}H NMR Titrations in CCl_4 at 295 K[a]

		global	microscopic		Δδ (ppm)					
complex	$\Delta G°$ (kJ mol^{-1})	K	K_1	K_2	OH	o	m	c	a	b
$\mathbf{A^O{\cdot}D}$	−11.3 ± 0.3	100 M^{-1}	100 M^{-1}		3.7	−0.1	−0.2		*0.0*	*0.1*
$\mathbf{A^OA^O{\cdot}D}$	−7.9 ± 0.6	50 M^{-1}	25 M^{-1}		*3.7*	*−0.2*	*−0.2*	0.1	0.1	0.1
$\mathbf{A^OA^O{\cdot}D_2}$	−16.1 ± 0.6	710 M^{-2}		27 M^{-1}	*2.3*	*−0.2*	*−0.2*	0.1	0.0	−0.1
$\mathbf{A^OA^O{\cdot}DD}$	−18.6 ± 0.3	1950 M^{-1}	1950 M^{-1}		2.4	−0.6	−0.2	*0.3*	*0.0*	*0.0*
$\mathbf{A^O{\cdot}DD}$	−13.5 ± 0.6	500 M^{-1}	250 M^{-1}		1.5	−0.2	−0.1		*0.1*	*0.1*
$\mathbf{A^O_2{\cdot}DD}$	−17.2 ± 0.6	1100 M^{-2}		4 M^{-1}	3.8	0.2	−0.3		*0.3*	*0.0*
$\mathbf{A^N{\cdot}D}$	−9.4 ± 0.3	47 M^{-1}	47 M^{-1}		*2.7*	*−0.1*	*−0.1*	0.2	0.2	0.2
$\mathbf{A^NA^N{\cdot}D}$	−9.5 ± 0.6	96 M^{-1}	48 M^{-1}		*0.5*	*0.0*	*−0.0*	0.0	0.0	
$\mathbf{A^NA^N{\cdot}D_2}$	−18.7 ± 0.6	2050 M^{-2}		43 M^{-1}	*1.4*	*−0.7*	*−0.8*	0.1	0.1	
$\mathbf{A^NA^N{\cdot}DD}$	−19.5 ± 0.3	2850 M^{-1}	2850 M^{-1}		*3.2*	*0.7*	*−0.1*	0.2	0.2	0.2
$\mathbf{A^N{\cdot}DD}$	−7.6 ± 0.6	44 M^{-1}	22 M^{-1}		3.6	0.2	0.0	*0.3*	*0.2*	*0.2*
$\mathbf{A^N_2{\cdot}DD}$	−15.2 ± 0.6	490 M^{-2}		22 M^{-1}	4.4	0.3	−0.1	*0.0*	*−0.3*	*−0.4*

[a] All titrations were repeated at least three times. K is the global association constant for formation of the complex from its components. For systems that can form both 1:1 and 2:1 complexes, K_1 is the statistically corrected microscopic association constant for formation of the 1:1 complex from its components, and K_2 is the statistically corrected microscopic association constant for formation of the 2:1 complex from the 1:1 complex. The global association constants for complexes $\mathbf{A^OA^O{\cdot}D}$, $\mathbf{A^O{\cdot}DD}$, $\mathbf{A^NA^N{\cdot}D}$, and $\mathbf{A^N{\cdot}DD}$ are quoted as macroscopic values that have not been statistically corrected, that is, $2K_1$. For these complexes, free energies are quoted using the statistically corrected microscopic association constants K_1. Errors in the Δδ values for the host are ±0.1 ppm, but the errors for the guest signals are larger (values in italics).

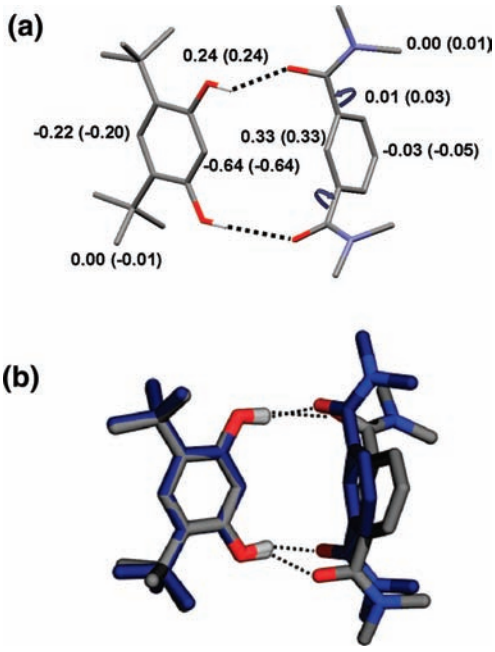

Figure 4. (a) Structure of the $\mathbf{A^OA^O{\cdot}DD}$ complex obtained from *Shifty* using the experimental complexation-induced changes in ^{1}H NMR chemical shift. The experimental Δδ values are shown with the calculated values from the structure optimization in brackets. The intermolecular orientation and position and the two torsion angles indicated were allowed to vary during the structure optimization process.[14] (b) Overlay of the structures obtained from *Shifty* (gray) and from molecular mechanics calculations using the OPLS force-field in Macromodel (blue).[10]

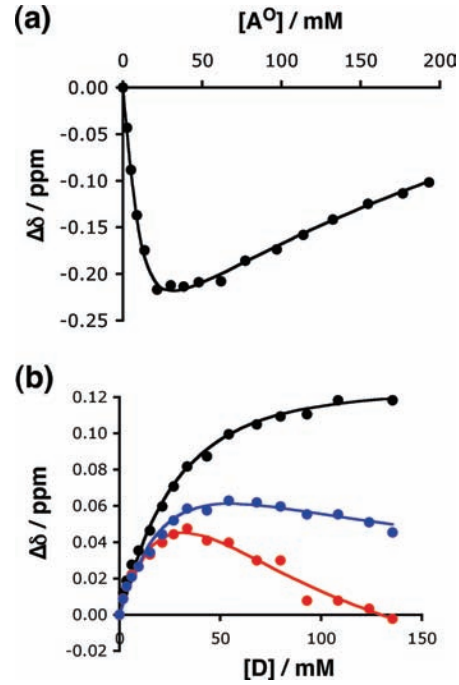

Figure 5. (a) Changes in the ^{1}H NMR chemical shift of the signal due to proton **o** in **DD** on addition of $\mathbf{A^O}$. The line shows the best fit to a 2:1 binding isotherm. (b) Changes in the ^{1}H NMR chemical shift of the signals due to protons **c** (black), **a** (blue), and **b** (red) in $\mathbf{A^OA^O}$ on addition of **D**. The lines show the best fit to a 2:1 binding isotherm.

previously.[14] The calculation converged to a well-defined structure, and the results are shown in Figure 4. The experimental structure is in close agreement with the structure calculated using molecular mechanics. The tilted geometry means that proton **o** of **DD** is located over the aromatic ring of the bisamide $\mathbf{A^OA^O}$, and this is the reason for the large negative Δδ value for this proton. The structures of the other complexes were also investigated using this method, but the singly H-bonded complexes are less constrained, and a large number of different H-bonded structures are consistent with the experimental data in all cases.

For the 2:1 complexes formed by the amide systems, the titration data show clear evidence that the two binding events are different (Figure 5). The changes in chemical shift for the signal due to proton **o** in **DD** suggest a difference in structure between $\mathbf{A^O{\cdot}DD}$ and $\mathbf{A^O_2{\cdot}DD}$. At the beginning of the titration, the signal moves upfield, which is consistent with the behavior of this signal in all of the other complexes (Table 1), but in the second phase of the titration, the signal moves downfield (Figure

(14) (a) Hunter, C. A.; Packer, M. J. *Chem.-Eur. J.* **1999**, *5*, 1891–1897. (b) Packer, M. J.; Zonta, C.; Hunter, C. A. *J. Magn. Reson.* **2003**, *162*, 102–112. (c) Gardner, M.; Guerin, A. J.; Hunter, C. A.; Michelsen, U.; Rotger, C. *New J. Chem.* **1999**, 309–316. (d) Hunter, C. A.; Low, C. M. R.; Packer, M. J.; Spey, S. E.; Vinter, J. G.; Vysotsky, M. O.; Zonta, C. *Angew. Chem., Int. Ed.* **2001**, *40*, 2678–2686. (e) Spitaleri, A.; Hunter, C. A.; McCabe, J. F.; Packer, M. J.; Cockroft, S. L. *CrystEngComm* **2004**, *6*, 489–493. (f) Hunter, C. A.; Spitaleri, A.; Tomas, S. *Chem. Commun.* **2005**, 3691–3693.

Table 2. Calculated and Experimental Association Constants for Formation of H-Bonded Complexes in CCl_4 at 295 K

complex	α^a	β^b	log K_{pred}	log K_{expt}
$\mathbf{A^O{\cdot}D}$	3.6	8.0	1.8	2.0
$\mathbf{A^OA^O{\cdot}D}$	3.6	7.0	1.4	1.4
$\mathbf{A^OA^O{\cdot}D_2}$	3.6	7.0	2.8	2.9
$\mathbf{A^OA^O{\cdot}DD}$	3.4	7.0	3.4	3.3
$\mathbf{A^O{\cdot}DD}$	3.4	8.0	1.5	2.4
$\mathbf{A^O_2{\cdot}DD}$	3.4	8.0	3.1	3.0
$\mathbf{A^N{\cdot}D}$	3.6	7.0	1.4	1.7
$\mathbf{A^NA^N{\cdot}D}$	3.6	7.0	1.4	1.7
$\mathbf{A^NA^N{\cdot}D_2}$	3.6	7.0	2.8	3.3
$\mathbf{A^NA^N{\cdot}DD}$	3.4	7.0	3.4	3.5
$\mathbf{A^N{\cdot}DD}$	3.4	7.0	1.2	1.3
$\mathbf{A^N_2{\cdot}DD}$	3.4	7.0	2.4	2.7

[a] These values were derived from literature values of α_2^H using the relationship $\alpha = 4.1(\alpha_2^H + 0.33)$. The value for **D** is based on the literature data for this compound, and the value for **DD** is based on the value for 2-*t*-butylphenol. The α values for phenol and 3-methoxyphenol are identical, so we assume that the resorcinol hydroxyl groups have little effect on each other.[12] [b] These values were derived from literature values of β_2^H using the relationship $\beta = 10.3$ ($\beta_2^H + 0.06$). The value for $\mathbf{A^O}$ is based on the literature data for *N*,*N*-dicyclohexyl benzamide, and the value for $\mathbf{A^OA^O}$ is based on the value for *N*,*N*-dicyclohexyl 4-nitrobenzamide, which probably exaggerates the substituent effect.[12] The values for $\mathbf{A^N}$ and $\mathbf{A^NA^N}$ are both based on the literature data for pyridine.[12] Data have not been reported for a suitable analogue of $\mathbf{A^NA^N}$, but the minimum on the AM1 molecular electrostatic potential surface of $\mathbf{A^NA^N}$ is practically identical to that found for $\mathbf{A^N}$, which suggests that the substituent effect is small in this compound. The experimental results in Table 1 confirm that the H-bond acceptor properties of $\mathbf{A^NA^N}$ and $\mathbf{A^N}$ are practically identical.

5a). The association constant for the first binding event (K_1 = 250 M^{-1}) is significantly larger than that for the second binding event (K_2 = 4 M^{-1}). The value K_1 is also significantly larger than $K(\mathbf{A^O{\cdot}D})$, which suggests that there are additional intermolecular interactions, for example, aromatic interactions, in the $\mathbf{A^O{\cdot}DD}$ complex that are lost again on formation of the $\mathbf{A^O_2{\cdot}DD}$ complex. This would account for the increase in K_1 and decrease in K_2. In the titration of $\mathbf{A^OA^O}$ with **D**, the signals due to protons **a** and **b** first move downfield then upfield during the titration, indicating that the $\mathbf{A^OA^O{\cdot}D}$ and $\mathbf{A^OA^O{\cdot}D_2}$ complexes also have different structural properties (Figure 5b). However, in this case, there is no difference in the microscopic association constants for the two binding events ($K_1 \approx K_2$). Although this behavior complicates analysis of the titration data, the peculiarities in the behavior of the 1:1 complexes, $\mathbf{A^O{\cdot}DD}$ and $\mathbf{A^OA^O{\cdot}D}$, do not affect the double mutant cycle and the determination of EM, which depends only on the overall stability of the 2:1 complexes, $\mathbf{A^O_2{\cdot}DD}$ and $\mathbf{A^OA^O{\cdot}D_2}$ (Figure 3, eq 2).

The stability constants in Table 1 show that there are significant substituent effects on the H-bond interactions in these systems. The microscopic association constants for formation of $\mathbf{A^OA^O{\cdot}D}$ from $\mathbf{A^OA^O}$ and **D** (25 M^{-1}) and for formation of $\mathbf{A^OA^O{\cdot}D_2}$ from $\mathbf{A^OA^O{\cdot}D}$ and **D** (27 M^{-1}) are both 4-fold lower than the association constant for formation of the reference $\mathbf{A^O{\cdot}D}$ complex (100 M^{-1}). This is due to the electron-withdrawing amide substituents that reduce the H-bond acceptor ability of the carbonyl groups in $\mathbf{A^OA^O}$ as compared to $\mathbf{A^O}$. The microscopic association constant for formation of each H-bond in the $\mathbf{A^O_2{\cdot}DD}$ complex ($\sqrt{K}$ = 33 M^{-1}) is 3-fold lower than the association constant for formation of the reference $\mathbf{A^O{\cdot}D}$ complex (100 M^{-1}). This substituent effect is consistent with the experimentally measured H-bond donor properties of phenol and 2-*t*-butyphenol, which indicate that **DD** is likely to be a slightly poorer H-bond donor than **D** (see Table 2). However, the double mutant cycle approach is specifically designed to quantify these effects and eliminate any contribution to the value of EM obtained using eq 2.

The behavior of the pyridine system was much simpler. Titrations were carried out with the H-bond acceptor as the host, except in the case of the $\mathbf{A^N_2{\cdot}DD}$ complex. No biphasic behavior was observed in any of the titrations, and systems with a 2:1 stoichiometry gave simple binding isotherms with similar microscopic association constants for the first and second binding event. The **OH** signal shows large downfield shifts in all of the complexes, indicative of H-bonding interactions. The stability constants in Table 1 show that there are no significant substituent effects on the H-bond interactions in complexes involving $\mathbf{A^NA^N}$. The microscopic association constants for formation of $\mathbf{A^NA^N{\cdot}D}$ from $\mathbf{A^NA^N}$ and **D** (48 M^{-1}) and for formation of $\mathbf{A^NA^N{\cdot}D_2}$ from $\mathbf{A^NA^N{\cdot}D}$ and **D** (43 M^{-1}) are the same as the association constant for formation of the reference $\mathbf{A^N{\cdot}D}$ complex (47 M^{-1}). The microscopic association constants for formation of $\mathbf{A^N{\cdot}DD}$ from $\mathbf{A^N}$ and **DD** (22 M^{-1}) and for formation of $\mathbf{A^N_2{\cdot}DD}$ from $\mathbf{A^N}$ and $\mathbf{A^N{\cdot}DD}$ (22 M^{-1}) are 2-fold lower than the association constant for formation of the reference $\mathbf{A^N{\cdot}D}$ complex (47 M^{-1}). This substituent effect is very similar to that observed for **DD** in the amide complexes. These systems therefore provide ideal cases for the determination of EM using the double mutant cycle in Figure 3 and eq 2, which corrects for the small substituent effects on the H-bond properties of the functional groups involved.

Evaluation of Cooperativity. Using eq 2, the value of EM for the intramolecular interaction in the doubly H-bonded complexes $\mathbf{AA{\cdot}DD}$ can be estimated at 12 ± 5 and 3 ± 1 M for the amide and pyridine systems, respectively. These values correspond to a free energy contribution of −6 and −3 (±1) kJ mol^{-1} arising from the intramolecular nature of the second H-bond interaction. Despite the differences in structure shown in Figure 1, the magnitude of the chelate cooperativity is similar in the two systems and consistent with the value of 6 kJ mol^{-1} that we have proposed as the free energy penalty associated with restricting biomolecular motion on formation of a 1:1 H-bonded complex.[2] A free energy penalty of 6 kJ mol^{-1} for an intermolecular interaction implies that for cooperative intramolecular interactions in well-organized complementary molecular assemblies the value of EM should be of the order 10 M, as observed in the complexes reported here.

We have previously shown that the stability of an intermolecular complex that contains a single H-bond interaction can be estimated reasonably well by eq 3.[15]

$$\Delta G^o = -(\alpha - \alpha_S)(\beta - \beta_S) + 6 \text{ kJ mol}^{-1} \qquad (3)$$

where α and β are the H-bond parameters for the functional groups that form the H-bond in the complex, and α_S and β_S are the corresponding parameters for the solvent.

The results for the doubly H-bonded complexes above suggest that this equation can be extended in a straightforward way to estimate the stability of a H-bonded complex that contains multiple interaction sites (eq 4).

$$\Delta G^o = -\sum_{\text{sites}} (\alpha - \alpha_S)(\beta - \beta_S) + 6(N - 1) \text{ kJ mol}^{-1} \qquad (4)$$

where N is the number of molecules involved in the complex, α and β are the functional group H-bond parameters for the

(15) Cook, J. L.; Hunter, C. A.; Low, C. M. R.; Perez-Velasco, A.; Vinter, J. G. *Angew. Chem., Int. Ed.* **2007**, *46*, 3706–3709.

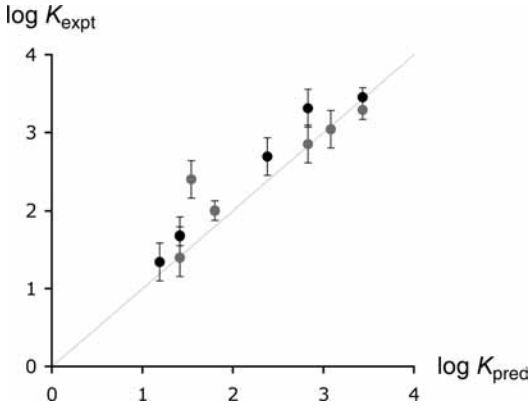

Figure 6. Correlation between the association constant estimated using eq 4 (K_{pred}) and the experimental values for the eight complexes in Table 1 (K_{expt}), showing the data for the amide complexes in gray and the pyridine complexes in black. The line corresponds to $y = x$. Excluding the anomalous $\mathbf{A^O \cdot DD}$ complex, the correlation coefficient between the calculated and experimental values of log K is $r^2 = 0.96$.

interactions formed in the complex, α_S and β_S are the corresponding parameters for the solvent, and the sum represents the sum over all intermolecular interaction sites.

In practice, factors that are known to impinge on effective molarities are likely to reduce the observed stability of a complex as compared to the theoretical value given by eq 4. Thus, flexible molecules that lose conformational degrees of freedom on complexation will form less stable complexes, as will systems where there is conformational strain or a mismatch in the geometry of the binding sites.[16] Nevertheless, eq 4 serves as a useful guide to the association constant that one can expect to achieve in a well-designed system. The eight complexes discussed above present different stoichiometries and numbers of interaction sites and serve as a simple test of eq 4. The H-bond parameters used for the functional groups involved are listed in Table 2. As discussed above, there are substituent effects on the H-bond properties of the functional groups, and so the H-bond parameters quoted in Table 2 are based on analogous literature compounds for which experimental data are available. The agreement between the association constants estimated using eq 4 and the experimental association constants is rather good in most cases (Table 2, Figure 6). The only major outlier is the $\mathbf{A^O \cdot DD}$ complex, which is the system that displays anomalous behavior in the ^{1}H NMR titration, as discussed above ($K_1 \gg K_2$). The experimental value of the association constant for this complex is an order of magnitude larger than that predicted by eq 4, which is indicative of the additional aromatic interactions that stabilize this complex.

Solvent Effects. To investigate the influence of the solvent on the cooperativity observed in the doubly H-bonded complexes, a further set of experiments was carried out in cyclohexane, 1,1,2,2-tetrachloroethane, and chloroform. Because of the complications and structural complexity encountered in titrations with the amide system in carbon tetrachloride, only the pyridine system was studied. The behavior of the complexes in the ^{1}H NMR titrations was very similar to that observed in carbon tetrachloride, and the results are collected in Table 3. As compared to carbon tetrachloride, the association constants

Table 3. Association Constants and Cooperativity Parameters from ^{1}H NMR Titrations in Various Solvents at 295 K[a]

solvent	complex	K	$\Delta G°$ (kJ mol^{-1})	$\Delta\Delta G°$ (kJ mol^{-1})	EM (M)
CCl_4	$\mathbf{A^N \cdot D}$	47 M^{-1}	-9.4 ± 0.3		
	$\mathbf{A^N A^N \cdot DD}$	2850 M^{-1}	-19.5 ± 0.3	-3 ± 1	3
	$\mathbf{A^N{}_2 \cdot DD}$	490 M^{-2}	-15.2 ± 0.6		
	$\mathbf{A^N A^N \cdot D_2}$	2050 M^{-2}	-18.7 ± 0.6		
C_6H_{12}	$\mathbf{A^N \cdot D}$	130 M^{-1}	-11.9 ± 0.3		
	$\mathbf{A^N A^N \cdot DD}$	7400 M^{-1}	-21.9 ± 0.4	-9 ± 1	33
	$\mathbf{A^N{}_2 \cdot DD}$	8500 M^{-2}	-22.2 ± 0.5		
	$\mathbf{A^N A^N \cdot D_2}$	220 M^{-2}	-13.2 ± 0.4		
$C_2H_2Cl_4$	$\mathbf{A^N \cdot D}$	24 M^{-1}	-7.8 ± 0.3		
	$\mathbf{A^N A^N \cdot DD}$	240 M^{-1}	-13.4 ± 0.4	-6 ± 1	12
	$\mathbf{A^N{}_2 \cdot DD}$	120 M^{-2}	-11.7 ± 0.3		
	$\mathbf{A^N A^N \cdot D_2}$	50 M^{-2}	-9.6 ± 0.3		
$CHCl_3$	$\mathbf{A^N \cdot D}$	25 M^{-1}	-7.8 ± 0.2		
	$\mathbf{A^N A^N \cdot DD}$	410 M^{-1}	-14.8 ± 0.5	-7 ± 1	20
	$\mathbf{A^N{}_2 \cdot DD}$	90 M^{-2}	-11.0 ± 0.3		
	$\mathbf{A^N A^N \cdot D_2}$	67 M^{-2}	-10.3 ± 0.3		

[a] All titrations were repeated at least three times. K is the global association constant for formation of the complex from its components.

are generally larger in cyclohexane and smaller in tetrachloroethane and chloroform. In most cases, there are small substituent effects, which are corrected for in the double mutant cycle, but in cyclohexane, the $\mathbf{A^N A^N \cdot D_2}$ complex showed an anomalously low association constant as compared to the reference complex $\mathbf{A^N \cdot D}$: the microscopic association constant for formation each H-bond in the $\mathbf{A^N A^N \cdot D_2}$ complex ($\sqrt{K} = 15$ M^{-1}) is 10-fold lower than the association constant for formation of the reference $\mathbf{A^N \cdot D}$ complex (130 M^{-1}). This result is responsible for the higher value of EM found in cyclohexane. Although the values of EM in Table 3 show some variation, they are similar in all four solvents, and given the errors and assumptions involved in these measurements, any further interpretation of the differences is not warranted. We conclude that for this range of solvents, there are no substantial solvent effects on chelate cooperativity, and the free energy benefit associated with the intramolecularity of a H-bond is between 3 and 9 kJ mol^{-1}. Note that this free energy contribution, $-RT$ ln(EM), is different from the net free energy benefit associated with formation of the intramolecular H-bond, $-RT$ ln(K EM). For the systems studied here, the complexes featuring intramolecular H-bonds are 6−12 kJ mol^{-1} more stable than the corresponding singly H-bonded complexes.

Conclusions

This article introduces the use of chemical double mutant cycles for the quantification of chelate cooperativity in multiply H-bonded complexes. The approach specifically deals with the effects of substituents, secondary interactions, and allosteric cooperativity on the free energy contributions from individual H-bond sites and allows dissection of the free energy contribution due to chelate cooperativity associated with the formation of intramolecular noncovalent interactions. Two different doubly H-bonded motifs and four different organic solvents were investigated, and the results were similar in all cases. The effective molarity for formation of intramolecular H-bonds is in the range 3−33 M for these systems. This corresponds to a free energy penalty of 3−9 kJ mol^{-1} for formation a bimolecular complex in solution, which is consistent with previous estimates of 6 kJ mol^{-1}.[2] The H-bond motifs in this work were chosen, because the molecular components are geometrically complementary and relatively rigid, which minimizes the effects of geometric strain and loss of conformational entropy on binding.

(16) (a) Bruice, T. C.; Lightstone, F. C. *Acc. Chem. Res.* **1999**, *32*, 127–136. (b) Cacciapaglia, R.; Di Stefano, S.; Mandolini, L. *Acc. Chem. Res.* **2004**, *37*, 113–122. (c) Kirby, A. *Adv. Phys. Org. Chem.* **1980**, *17*, 183.

In addition, the H-bonding sites are sufficiently well-separated to avoid the complications of secondary electrostatic interactions. Thus, the effective molarities for these systems are likely to be close to the upper limit for multiply H-bonded architectures and are significantly higher than the values that we reported recently for some related but more flexible complexes.[17] Used in conjunction with the H-bond parameters, α and β, the free energy penalty of 6 kJ mol^{-1} for formation of a bimolecular complex for perfectly complementary intramolecular interactions can be used to make a reasonable estimate of the stability constant for formation of a multiply H-bonded complex.

Experimental Section

^{1}H NMR Titrations. ^{1}H NMR titrations were carried out by preparing a 3 mL sample of the host at known concentration (0.1−10 mM) in CCl_4, cyclohexane, 1,1,2,2-tetrachloroethane-d_2, or chloroform-*d*. For the nondeuterated solvents, CCl_4 and cyclohexane, a capillary with D_2O was used inside the NMR tube as a lock signal, and a solvent suppression pulse sequence was used in the cyclohexane experiments. 0.6 mL of the host solution was removed, put in the NMR tube, and a ^{1}H NMR spectrum was recorded. An accurately weighed sample of the guest was dissolved in 2 mL of the host solution (so that the concentration of host remained constant during the titration). The concentration of guest was 10−100 times larger than that of host. Aliquots of the guest solution were added successively to the NMR tube containing the host solution, and the ^{1}H NMR spectrum was recorded after each addition. Changes in chemical shift for the proton signals were analyzed using purpose written software. This allowed calculation of the association constant for all of the complexes. Dilution studies in CCl_4 indicated that aggregation was insignificant at the concentrations used. However, dimerization of **D** was taken into account to fit the data for complex $\mathbf{A^NA^N \cdot D_2}$.[18] Dimerization does not affect the value of the association constant, but the chemical shift of the **OH** proton changes dramatically at high concentrations, and this affects the guest limiting changes in chemical shift.

NMR Structure Determination. NMR structure determinations were carried out using the *Shifty* software described in detail elsewhere.[15] The molecules were built in XED 2.8 using standard bond lengths and angles and were energy minimized.[19] A genetic algorithm was used to optimize the conformation of the complex so that the calculated $\Delta\delta$ values matched the experimental values as closely as possible. The conformational search allowed intermolecular translations of ±5 Å and intermolecular rotations of ±180°, as well as intramolecular torsional changes of ±180° for the bonds highlighted in Figure 4. The van der Waal clashes were penalized at distances less than 2 Å for intermolecular clashes and 1 Å for intramolecular clashes for non-hydrogen atoms. In all cases, 20 different runs using random starting points were carried out. All solutions with rmsd values less than 0.02 ppm were collected. Each run was carried out in five steps, progressively reducing each dimension of the search space by a factor of 2. For each step, the population size was set to 500 and number of generations to 1000. Each calculation (20 runs) took about 6 h on a DELL-Linux cluster with 12 dual processor INTEL Pentium IV 3.0 GHz nodes.

Acknowledgment. We thank the EPSRC for funding.

Supporting Information Available: Synthetic details. This material is available free of charge via the Internet at http://pubs.acs.org.

JA9083495

(17) Hunter, C. A.; Ihekwaba, N.; Misuraca, M. C.; Segarra-Maset, M. D.; Turega, S. M. *Chem. Commun.* **2009**, 3964–3966.
(18) Hunter, C. A.; Jones, P. S.; Tiger, P.; Tomas, S. *Chem.-Eur. J.* **2002**, *8*, 5435–5446.
(19) Vinter, J. G. *J. Comput.-Aided Mol. Des.* **1994**, *8*, 653–668.